



Structural and optical properties of ZnO nanoparticle thin films deposited by sol gel method

Nasser K.Hejazy

Al-Quds Open University, Gaza Branch, Department of Education, Gaza Strip, Gaza, (PALESTINE)

E-mail: naserkhejazy@hotmail.com

ABSTRACT

Nanocrystalline ZnO thin films are deposited on glass substrates by by sol gel process. The crystalline structure, morphology and size were determined by X-ray diffraction (XRD) and transmission electron microscopy (TEM). The X-ray diffraction results indicated that ZnO nanoparticles have a hexagonal wurtzite structure and average particle size is about 4 nm. Photoluminescence spectra showed two peaks which were in the UV emission centered at 375 nm, and visible emission centered at 475 nm. © 2015 Trade Science Inc. - INDIA

KEYWORDS

Structural;
Optical;
Properties;
ZnO;
Nanoparticles;
Sol gel.

INTRODUCTION

ZnO is a II-IV semiconductor compound and has a direct bandgap around 3.2-3.37eV in 300K with a high exciton binding energy of 60 meV and is a wide bandgap semiconductor. ZnO thin films are important materials^[1], due to their unique properties such as low electric resistance, high transparency in the visible light, piezoelectricity, high voltage-current nonlinearity and chemical stability^[2] and their applications are in bulk acoustic wave solar cells, transparent electrodes, blue UV light emitter device and gas sensors^{[3]-[8]}. Various chemical methods have been developed to prepare nanoparticles of different materials of interest. Most of the ZnO crystals have been synthesized by traditional high temperature solid state method in which, it is difficult to control the particle properties and also energy consuming. ZnO nanoparticles can be prepared on a

large scale at low cost by simple solution based method, such as chemical precipitation, sol-gel synthesis, and hydrothermal reaction^[9-14]. Among these methods, the hydrolysis of zinc acetate salts in alcohol has been extensively investigated to obtain monodispersed ZnO nanoparticles^[15].

Several deposition techniques have been used to grow the ZnO thin films which include thermal evaporation^[16], sputtering^[17,18], chemical vapor deposition^[19], spray pyrolysis^[20-22], the sol-gel method^[23], dip coating^[24]. In the present investigation we have used the sol-gel technique to deposit the ZnO thin films as this technique is being simple, inexpensive in fabrication of a large number of samples, easier for composition control, with accurately controlled mole ratio, high solubility, better homogeneity, and lower processing temperature and a general advantage of large area deposition and any suitable thickness of the film.

Full Paper

In this work, a sol-gel method to deposit ZnO nanoparticle (NP) thin films on the glass substrates has been investigated. The structural, optical, and electrical properties of the films were characterized by X-ray diffraction (XRD), photoluminescence (PL), UV-vis spectrometry

EXPERIMENTAL

ZnO sol was prepared using zinc acetate dihydrate ($\text{Zn}(\text{CH}_3\text{COO})_2 \cdot 2\text{H}_2\text{O}$, Merck) as the starting material, 2-methoxyethanol ($\text{C}_3\text{H}_8\text{O}_2$, Sigma-Aldrich) as the solvent, and monoethanolamine (MEA, $\text{C}_2\text{H}_7\text{NO}$, Merck) as the sol stabilizer. The concentration of zinc acetate was 0.4 M and the molar ratio of MEA to zinc acetate was maintained at 1.0. Solution was stirred on a hot plate stirrer with applied temperature of 80°C for 1 hour to yield a homogenous solution. The resultant clear solution was aged for 24 hours at room temperature. Glass slides were cut into 2×2 squares and cleaned using acetone, methanol and de-ionized water in an ultrasonic bath for 10 minutes each. The sol was dropped onto the spinning glass substrate with a rotation speed of 3000 rpm for 60 seconds. Each coating was dried at 150°C for 10 minutes to remove the solvent and organic residues. The film was then annealed in air at a temperature of 500°C for 30 minute

each layer. The process from coating to annealing was repeated 2 to 4 times to produce different thickness of the films.

The films thicknesses were measured using a surface profiler (model: KLA-Tencor).

The UV absorption spectra were taken with a Hewlett Packard 8453 spectrometer. The fluorescence measurements were done with a Perkin-Elmer LS 50B luminescence spectrometer. The AFM images of the films were acquired using a NTEGRA scanning probe microscope. The transmission electron microscopy (TEM) analysis was done with a Tecnai F300 transmission electron microscope, images taken after suspending in 95% ethanol. Crystal structure identification and crystal size analysis were carried out by X-ray diffraction XDS 2000, Scintac Inc., USA with $\text{CuK}\alpha$ radiation source, and scan rate of $2^\circ/\text{min}$.

RESULT AND DISCUSSION

All the films were found to be almost clear and transparent in physical appearance, and well adherent to the glass substrates. The as-deposited films were annealed at 500°C for 1h to obtain highly uniform crystalline films. The film thicknesses were found to be in the range 42–43 nm. Figure 1 shows

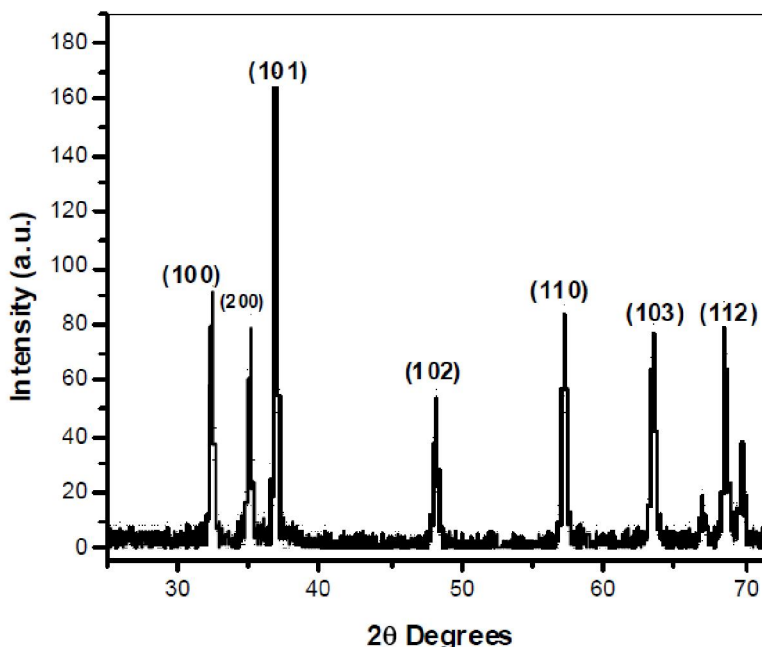


Figure 1 : XRD diffraction pattern of the ZnO nanoparticle thin films

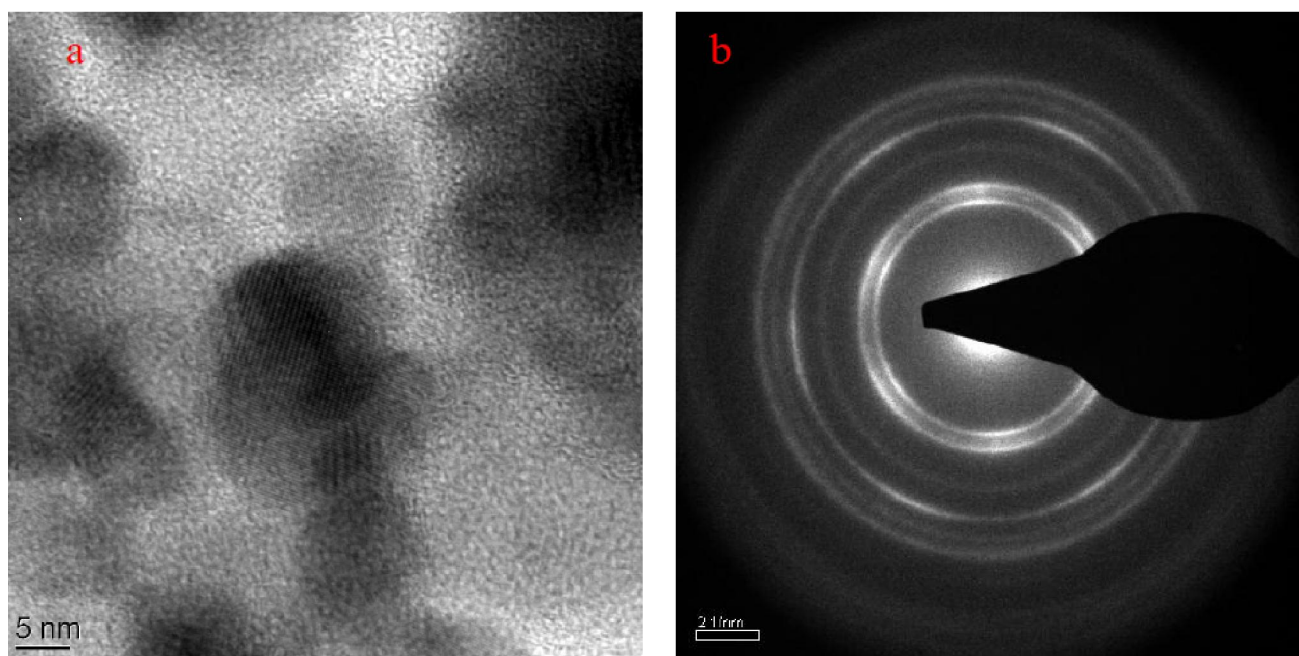


Figure 2(a,b) : TEM micrograph and selected area electron diffraction (SAED) pattern and of ZnO nanoparticle thin film

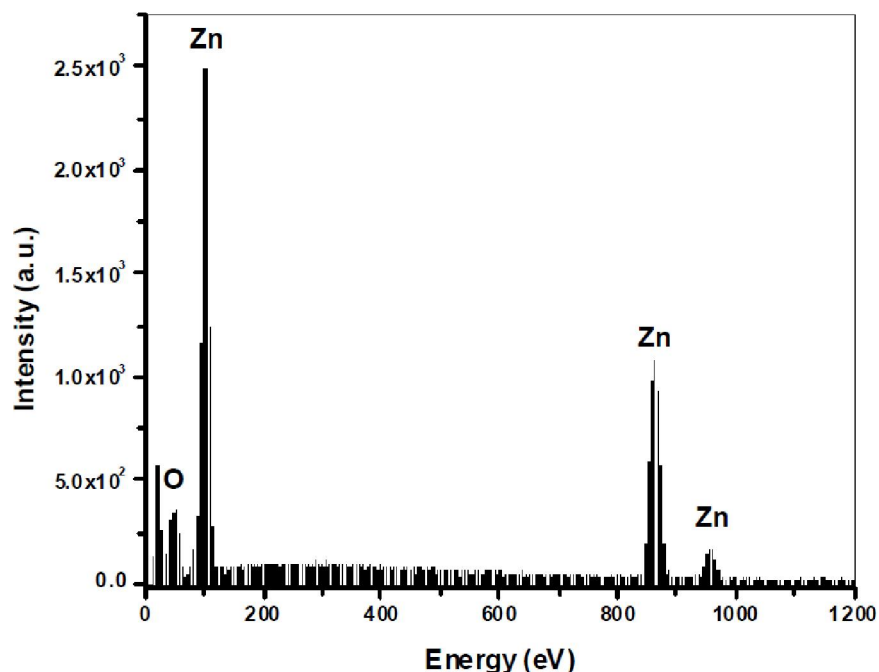


Figure 3 : EADX spectrum of the ZnO nanoparticle thin films.

the XRD spectra of the ZnO nanoparticle thin films. The observed XRD patterns have been found to match with JCPDS card (zinc oxide, 05-0664). XRD analyses confirm that all the films are polycrystalline zinc oxide possessing hexagonal wurtzite structure. XRD spectra also allowed for the calculation of crystallite size. The Scherrer formula $D = k\lambda/B \cos\theta$, where D is the particle size, k is a con-

stant of 0.9, λ is the X-ray wavelength, θ is the Bragg's angle in radians, and B is the full width at half maximum of the peak in radians was used to calculate crystallite size. The seven most prominent peaks (100), (002), (101), (102), (110), (103), and (112) were used in the calculation (Figure 1). Using this equation, it was found that average particle size of the sample was approximately 5 nm.

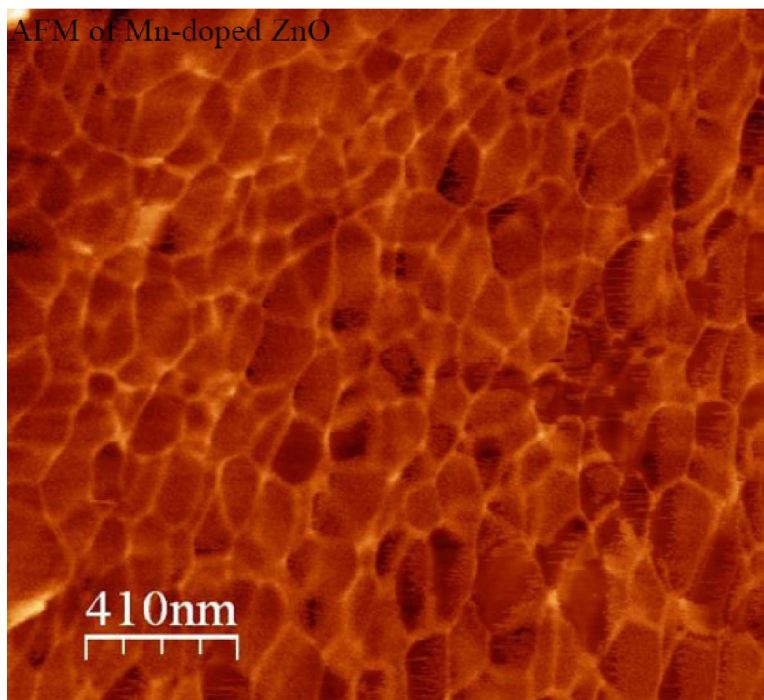


Figure 4 : AFM image of ZnO nanoparticle film.

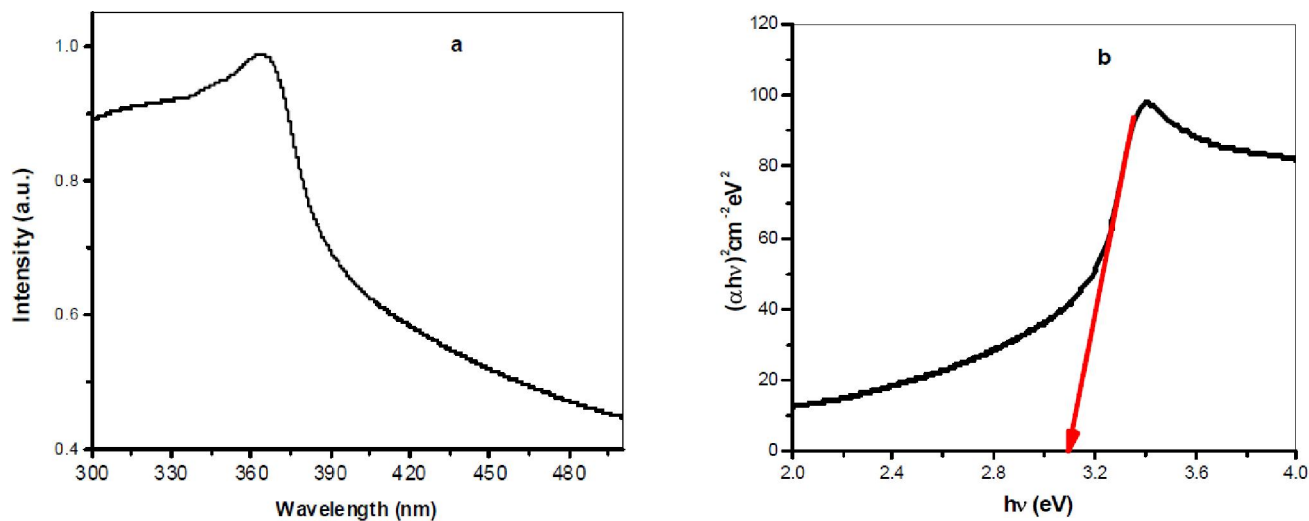


Figure 5 (a,b) : UV-vis spectra and optical band gap spectra of ZnO nanoparticle thin film.

Figure 2(a,b) shows the TEM micrograph and selected area electron diffraction (SAED) pattern and of ZnO nanoparticle thin film after sonication for 10 min. TEM micrographs of the ZnO thin film (Figure 2a) showed nearly spherical nanoparticles with an average particle size of 4 nm. This is consistent with estimated grain size (4 nm) from the XRD peak broadening. Figure 2b shows the representative selected area electron diffraction (SAED) pattern for ZnO nanoparticle thin film. This SAED patterns are indexed to the wurtzite ZnO structure,

consistent with above XRD result.

The EDAX Study of the prepared sample is shown in Figure 3. This shows that the sample contains only zinc and oxygen and no other impurity are present in the sample.

An atomic force microscope (AFM) was used to measure the surface roughness of films over $2\ \mu\text{m} \times 2\ \mu\text{m}$ area in contact mode. Figure 4 shows the AFM image of ZnO nanoparticle film. The topography image Figure 4 confirms the surface smoothness and the surface composed of hexagonal nanoparticles

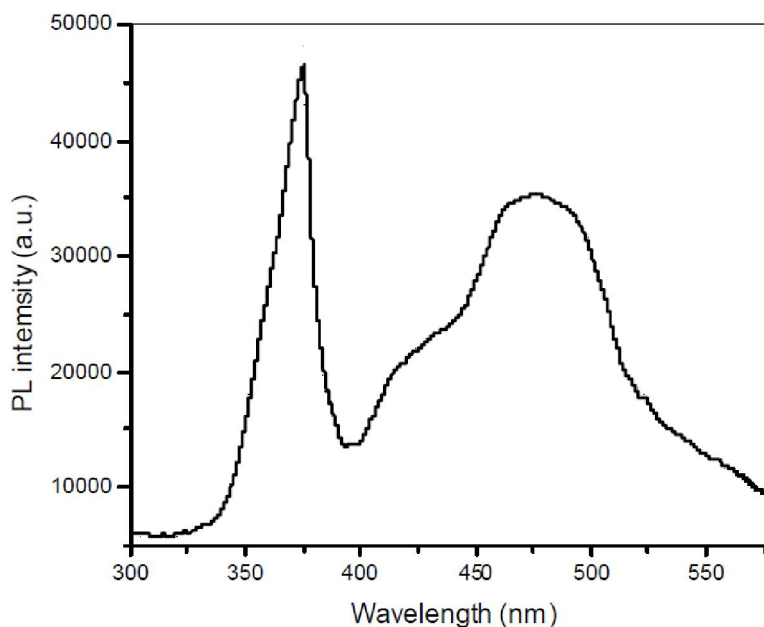


Figure 6 : PL spectrum of ZnO nanoparticle thin film.

which is in good agreement with the result of XRD analysis of ZnO nanoparticle thin film.

The optical properties of the ZnO nanoparticle thin film were studied by UV–Vis absorption spectroscopy. Figure 5a shows the UV-vis spectra of ZnO nanoparticle thin film at room temperature. The exciton absorption at 360 nm is observed in the absorption spectrum. When photons of higher energy are larger than band gap of the semiconductor, an electron is transferred from the valence band to the conduction band where there occurs an abrupt increase in the absorbency of the material to the wavelength corresponding to the band gap energy. The relation between the incident photon energy ($h\nu$) and the absorption coefficient (α) is given by the following relation:

$$(\alpha h\nu)^{\frac{1}{n}} = A(h\nu - E_g) \quad (1)$$

where A is the constant and E_g is the band gap energy of the material and the exponent n depends on the type of transition. For direct allowed transition $n= 1/2$, for indirect allowed transition $n= 2$, for direct forbidden $n= 3/2$ and for indirect forbidden $n= 3$. Direct band gap of the samples are calculated by plotting $(\alpha h\nu)^2$ versus $h\nu$ and then extrapolating the straight portion of the curve on the $h\nu$ axis at $\alpha = 0$ as shown in Figure 5b.

The band gap value of ZnO thin film is found to be 3.10 eV. These values are in good agreement with

the values reported by others^[25]. This red shift of the band gap energy is due to agglomeration of the nanocrystallites into larger crystallites as reported by various authors in different literatures.

The PL spectra of ZnO colloids were measured at room temperature with excitation at a wavelength of 320 nm. Figure 6 shows the PL spectrum of ZnO nanoparticle thin film. The PL spectra of as-prepared ZnO NPs showed two emission peaks: one is located around 375 nm (3.31 eV) in the ultraviolet region; the other is located at around 475 nm (2.61 eV) in the visible region (Figure 4). One was the near-band-edge emission in the UV range, which was attributed to free-exciton recombination, and the other one was a deep-level emission (DLE) mostly in the green and partly in the yellow and red spectral regions, which was produced by the transition of excited optical centers from the deep level to the valence level, such deep-level emission being usually accompanied by the presence of structural defects and impurities^[26,27].

CONCLUSION

ZnO nanoparticle thin films have been deposited using a sol-gel spin coating method on glass substrates. XRD and TEM morphological analysis showed that the ZnO nanoparticles had regularly

Full Paper

spherical particle with a size of 5 nm. Photoluminescence spectra showed two peaks which were in the UV emission centered at 360 nm, and visible emission centered at 580 nm.

REFERENCES

- [1] Talaat M.Hammad, Jamil K.Salem, Roger G.Harrison; *NANO*, **4**, 225 (2009).
- [2] Talaat M.Hammad, Jamil K.Salem, Roger G.Harrison; *Superlattices and Microstructures*, **47**, 335-340 (2010).
- [3] Talaat M.hammad, Jamil K.Salem; *J.Nanopar.Res.*, **13**, 2205 (2011).
- [4] Jamil K.Salem.Talaat M.Hammad, Roger G.Harrison; *J.Mater.Sci.: Mater Electron*, DOI 10.1007/s10854-012-0994-0, (2012).
- [5] Talaat M.Hammad, Jamil K.Salem, Roger G.Harrison; *Rev.Adv.Mater.Sci.*, **22**, 74-80 (2009).
- [6] Jamil K.Salem, Talaat M.Hammad, Roger G.Harrison; *International Journal of Nanoscience*, **8**, 465 (2009).
- [7] Jamil K.Salem, Talaat M.Hammad; *Journal of Materials Science and Engineering*, **3**, 38 (2009).
- [8] Talaat M.hammad, Jamil K.Salem; *J.Nanopar.Res.*, **13**, 2205 (2011).
- [9] T.M.Hammad, S.Griesing, M.Wotocek, S.Kuhn, R.Hempelmann, U.Hartmann, J.K.Salem; *Applied Nanoscience*, DOI 10.1007/s13204-012-0089-5, (2012).
- [10] Talaat.M.Hammad, Jamil.K.Salem, Roger G.Harrison, Rolf.Hempelmann, Nasser K.Hejazy; *J Mater Sci.: Mater Electron*, **24**, 2846–2852 (2013).
- [11] D.W.Bhnmann, C.Kormann, M.R.Hoffmann; *J.Phys.Chem.*, **91**, 3789 (1987).
- [12] Z.Hui, Y.Deren, M.Xiangyang, J.Yujie, X.Jin; *Nanotechnology.*, **15**, 622 (2004).
- [13] J.Zhang, L.D.Sun, J.L.Yin; *Chem.Mater.*, **14**, 4172 (2002).
- [14] W.J.Li, E.W.Shi, Z.W.Yin; *J.Mater.Sci.Lett.*, **20**, 1381 (2001).
- [15] Yuntao Li, Richard D.Yang, S.Tripathy, H.J.Sue, N.Miyatake, R.Nishimura; *Mater.Res. Soc.Symp.Proc.*, **829**, B8.4.1 (2005).
- [16] E.A.Meulenkamp; *J.Phys.Chem.B*, **102**, 5566 (1998).
- [17] A.Van Dijken, E.A.Meulenkamp, D.Vanmaekelbergh, A.Meijerink; *J.Lumin.*, **90**, 123-128 (2000).
- [18] T.M.Hammad, S.Griesing, M.Wotocek, S.Kuhn, R.Hempelmann, U.Hartmann, J.K.Salem ; *Int.J.Nanoparticles*, **6**, 324-336 (2013).
- [19] N.Bouhssira, S.Abed, E.Tomasella, J.Cellier, A.Mosbah, M.S.Aida et al. ; *Applied Surface Science*, **252**, 5594–5597.
- [20] WJamil K.Salem, Talaat M.Hammad, Mohammed Abu Draaz, S.Kuhn, R.Hempelmann; *J.Mater Sci.: Mater Electron*, **25**, 2177-2182 (2014).
- [21] Y.Z.Tsai, N.F.Wang, C.L.Tsai; *Thin Solid Films*, **518**, 4955–4959 (2010).
- [22] Jamil K.Salem, Talaat M.Hammad, S.Kuhn, Issa Nahal; Mohammed Abu Draaz, Naser K.Hejazy, R.Hempelmann, *J.Mater Sci.: Mater Electron*, **25**, 5188–5194 (2014).
- [23] A.Ashour, M.A.Kaid, N.Z.El-Sayed, A.A.Ibrahim; *Applied Surface Science*, **252**, 7844–7848 (2006).
- [24] L.A.Patil, A.R.Bari, M.D.Shinde, Vinita Deo; *Sensors and Actuators B*, **149**, 79–86 (2010).
- [25] M.T.Mohammad, A.A.Hashim, M.H.Al Maamory; *Materials Chemistry and Physics*, **99**, 382–387 (2006).
- [26] L.Znaidi; *Materials Science and Engineering B*, **174**, 18–30 (2010).
- [27] X.L.Cheng, H.Zhao, L.H.Huo, S.Gao, J.G.Zhao; *Sensors and Actuators B*, **102**, 248–252 (2004).
- [28] R.Y.Hong, J.H.Li, L.L.Chen, D.Q.Liu, H.Z.Li, Y.Zheng, J.Ding; *Powder Technol.*, **189**, 426 (2009).
- [29] Jared M.Hancock, William M.Rankin, Talaat M.Hamad, Jamil S.Salem, Karine Chesnel, Roger G.Harrison; *Journal of Nanoscience and Nanotechnology*, **15**(5), 3809-3815.
- [30] T.Hammad; *International Journal of Modern Physics B*, **20**, 3357 (2006).